

10-4-2010

Ferroelectricity in Non-Stoichiometric SrTiO₃ Films Studied by Ultraviolet Raman Spectroscopy

Dmitri A. Tenne
Boise State University

A. K. Farrar
Boise State University

Ferroelectricity in non-stoichiometric SrTiO₃ films studied by ultraviolet Raman spectroscopy

D. A. Tenne,^{1, a)} A. K. Farrar,¹ C. M. Brooks,^{2, 3} T. Heeg,³ J. Schubert,⁴ H. W. Jang,⁵ C. W. Bark,⁵ C. M. Folkman,⁵ C. B. Eom,⁵ and D. G. Schlom³

¹⁾*Department of Physics, Boise State University, 1910 University Dr., Boise, ID 83725-1570, USA*

²⁾*Department of Materials Science and Engineering, The Pennsylvania State University, University Park, PA 16802-5005, USA*

³⁾*Department of Materials Science and Engineering, Cornell University, Ithaca, NY 14853-1501, USA*

⁴⁾*Institute of Bio and Nanosystems, JARA-Fundamentals of Future Information Technologies, Research Centre Jülich, D-52425 Jülich, Germany*

⁵⁾*Department of Materials Science and Engineering, University of Wisconsin, Madison, Wisconsin 53706, USA*

(Dated: 6 October 2010)

Homoepitaxial Sr_{1+x}TiO_{3+δ} films with $-0.2 \leq x \leq 0.25$ grown by reactive molecular-beam epitaxy on SrTiO₃ (001) substrates have been studied by ultraviolet Raman spectroscopy. Non-stoichiometry for strontium-deficient compositions leads to the appearance of strong first-order Raman scattering at low temperatures, which decreases with increasing temperature and disappears at about 350 K. This indicates the appearance of a spontaneous polarization with a paraelectric-to-ferroelectric transition temperature above room temperature. Strontium-rich samples also show a strong first-order Raman signal, but the peaks are significantly broader and exhibit a less pronounced temperature dependence, indicating a stronger contribution of the disorder-activated mechanism in Raman scattering.

PACS numbers: 77.55.fp, 77.80.bg, 78.30.Hv, 63.20.-e

SrTiO₃ is a well known incipient ferroelectric, and in bulk remains paraelectric down to 0.3 K.¹ Slight perturbations in the lattice structure can, however, break the delicate balance of forces and lead to the appearance of ferroelectric polarization. This perturbation can come from various sources such as strain,²⁻⁵ doping,⁶⁻⁸ or even oxygen isotope substitution.⁹ Here we focus on the effect of Sr/Ti non-stoichiometry in homoepitaxial SrTiO₃ thin films. Specifically of interest is how variation in stoichiometry affects the phonons and their activity in Raman spectra resulting from the ferroelectric phase transitions. Raman spectroscopy is a powerful tool for probing lattice vibrations. For thin films of wide band gap materials such as SrTiO₃, excitation using ultraviolet (UV) light is preferable, since UV light with energy above the band gap (3.2 eV for SrTiO₃ at 300 K) is absorbed, and therefore the substrate signal is strongly suppressed allowing measurement of spectra from ferroelectric films as thin as a few nanometers.^{10,11} In this paper, we apply UV Raman spectroscopy to study ferroelectricity in non-stoichiometric (both strontium-rich and strontium-deficient) homoepitaxial SrTiO₃ films.

The 100 nm-thick films were grown by molecular-beam epitaxy (MBE) on stoichiometric, TiO₂-terminated (001) SrTiO₃ substrates at 650°C in a background pressure of 5.0×10^{-7} Torr of ultra-high purity molecular oxygen. Growth was monitored by reflection high-energy

electron diffraction. Six Sr_{1+x}TiO_{3+δ} films were studied; nominal compositions x varied from -0.2 to 0.3, including a stoichiometric film, $x = 0$. The Sr/Ti concentration ratios $(1 + x)$ were determined by Rutherford backscattering spectrometry (RBS) to be 0.786, 0.905, 0.97, 1.02, 1.19, and 1.24, resulting in x values -0.214, -0.095, -0.03, 0.02, 0.19, and 0.24 (± 0.04), close to the nominal ones. There may be a certain amount of oxygen non-stoichiometry δ , but the oxygen concentration in the films is difficult to determine by RBS due to the low atomic mass of oxygen. The details of growth and structural characterization by x-ray diffraction (XRD) and scanning transmission electron microscopy (STEM) have been reported elsewhere¹². According to STEM images, the strontium deficient films appear to have a disordered structure (randomly distributed defects); no secondary phases like TiO₂ were detected. In the strontium excess films, the Ruddlesden-Popper planar faults appear.¹² Both Sr-deficient and Sr-rich films have shown an expansion along the c axis; the c lattice parameters determined by XRD were 3.94, 3.915, 3.905, 3.92, 3.96, and 4.02 Å, respectively, for the compositions listed above.¹² Since the films were homoepitaxial, any effect of substrate-induced strain should be negligible. Also, spectra of nominally stoichiometric SrTiO₃ films grown by pulsed-laser deposition (PLD) on SrTiO₃ substrates with and without SrRuO₃ buffer layers were measured. The PLD growth details were reported elsewhere.¹³

Raman spectra were recorded using a Horiba Jobin Yvon T64000 triple spectrometer equipped with a liquid-nitrogen-cooled multichannel charge-coupled device de-

^{a)}Electronic mail: dmitritenne@boisestate.edu

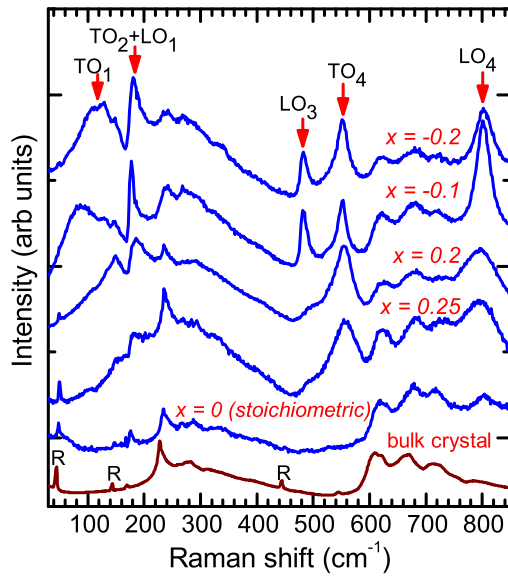


FIG. 1. (Color online) Raman spectra of $\text{Sr}_{1+x}\text{TiO}_{3+\delta}$ films and a bulk SrTiO_3 crystal at 10 K. Arrows mark the first-order SrTiO_3 phonon peaks. Symbols "R" label the structural modes due to the rotation of the Ti-O octahedra

tector. Spectra were recorded in backscattering geometry in the temperature range 10–450 K using a variable temperature closed cycle He cryostat. For excitation, the 325 nm He-Cd laser line was used with a power density of 0.5 W/mm^2 at the sample surface, low enough to avoid any noticeable local heating.¹⁴

SrTiO_3 is a cubic perovskite-type crystal having 12 optical phonon modes. All phonons are of an odd symmetry with respect to the inversion, hence inactive in the first-order Raman scattering. Raman spectrum of bulk SrTiO_3 contains only the second order (two-phonon) features.¹⁵ A breakdown in the inversion symmetry of the crystal (e.g., due to a ferroelectric distortion) leads to the appearance of the first-order peaks Raman spectra.

Figure 1 shows Raman spectra of a bulk SrTiO_3 crystal, the MBE-grown stoichiometric film, and non-stoichiometric films at 10 K. The stoichiometric film's spectrum is similar to bulk SrTiO_3 with broad second order peaks. The structural modes at 44, 144, 445 cm^{-1} (labelled R in Fig. 1) present in the low-temperature spectra are due to the antiferrodistortive cubic-tetragonal phase transition, which occurs at 105 K and involves the rotation of the Ti-O octahedra.¹⁶ The resulting tetragonal structure $4/mmm$ is still centrosymmetric and the fundamental SrTiO_3 phonons remain Raman inactive. In contrast, the non-stoichiometric films exhibit intensive first-order peaks of the fundamental SrTiO_3 phonons, indicative of a breakdown in inversion symmetry. The spectral features that we focus on are TO_1 (the soft mode) at $85\text{--}120 \text{ cm}^{-1}$, and the hard modes TO_2+LO_1 (these two modes have very close frequencies), LO_3 , TO_4 , and LO_4 at 180, 480, 550, and 800 cm^{-1} , respectively.

Variable temperature spectra of strontium-deficient

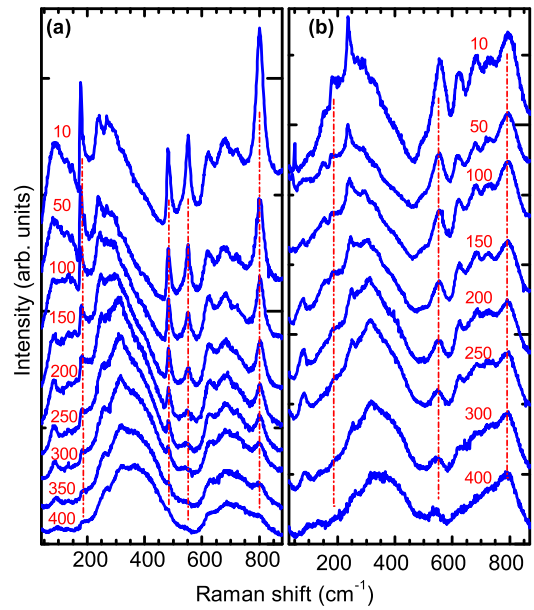


FIG. 2. (Color online) Variable-temperature Raman spectra of a Sr-deficient $\text{Sr}_{0.9}\text{TiO}_{3+\delta}$ film (a) and a Sr-rich $\text{Sr}_{1.25}\text{TiO}_{3+\delta}$ film (b). Numbers above the spectra indicate temperatures in K. The vertical dashed-dotted lines are guides for the eye showing the first-order SrTiO_3 phonon peaks.

films (Fig. 2(a)) showed these peaks decreasing and disappearing at $\sim 350 \text{ K}$. The complete disappearance of the first-order Raman peaks at higher temperatures indicates that the breakdown of the inversion symmetry selection rules cannot be attributed to lattice defects alone. If the first-order Raman scattering is defect-induced, it should be observed at higher temperatures as well. At higher temperatures (above 350 K), however, the spectra of strontium-deficient films are the same as stoichiometric SrTiO_3 . The observed behavior indicates the appearance of spontaneous polarization in the strontium-deficient films. Considering the temperature evolution of the spectra of strontium-rich films (Fig. 2(b)), one can notice a different behavior: even at low temperatures the phonon peaks are broad (about twice as broad compared to the strontium-deficient films), and they do not disappear even at high temperatures. This indicates a stronger contribution of the defect-induced mechanism in Raman scattering in the strontium-rich films.

The breakdown of the symmetry selection rules has been previously observed in Raman scattering from SrTiO_3 films grown by PLD,¹⁷ and attributed to polar nanoregions associated with oxygen vacancies¹⁷ or dipole moments associated with polar grain boundaries in polycrystalline or textured samples.¹⁸ The samples studied here are single-crystalline films having no grain boundaries, so this effect is not present. Later studies of intentionally oxygen-reduced bulk SrTiO_3 showed that oxygen vacancies alone are unlikely to cause the observed effect, and should also lead to the appearance of additional peaks, that are not present in the thin film spectra.¹⁹

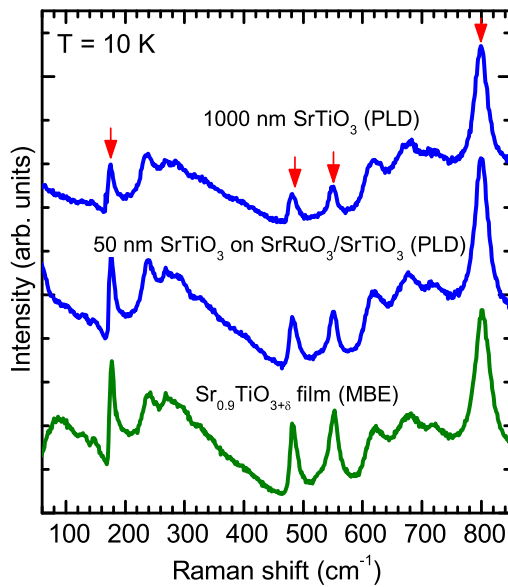


FIG. 3. (Color online) Raman spectra of the strontium-deficient MBE-grown film ($\text{Sr}_{0.9}\text{TiO}_{3+\delta}$) and two nominally stoichiometric SrTiO_3 films grown by PLD on SrTiO_3 substrates with and without SrRuO_3 buffer layers. Arrows indicate the first-order peaks of the SrTiO_3 optical phonons.

Even if oxygen vacancies play a role, it must be in combination with other non-stoichiometry or defects.

Figure 3 shows Raman spectra of strontium-deficient film and two nominally stoichiometric PLD-grown SrTiO_3 films on SrTiO_3 substrates without and with SrRuO_3 buffer layers. The latter films (with SrRuO_3 bottom electrodes) were proved to be ferroelectric by a combination of techniques including the polarization hysteresis loops measured by piezoresponse force microscopy.¹³ The shape and temperature evolution of Raman spectra from SrTiO_3 films with and without SrRuO_3 contact layers are essentially the same. This indicates that thin coherently strained SrRuO_3 layers following the lattice parameter of the SrTiO_3 substrate have no noticeable effect on the properties of SrTiO_3 films. The spectra of the strontium-deficient films studied here are remarkably similar to the spectra of the PLD-grown ferroelectric SrTiO_3 in terms of both the first-order Raman peaks (which are slightly stronger in the strontium-deficient films) and their temperature evolution (Fig. 3). This result supports the suggestion that relatively small amounts of cation non-stoichiometry, which were demonstrated to occur even in nominally stoichiometric PLD-grown samples,^{20,21} can lead to the appearance of polar nanoregions and relaxor-like ferroelectricity, as reported by Jang *et al.*¹³

In summary, Sr/Ti non-stoichiometry in homoepitaxial SrTiO_3 films leads to the appearance of first-order peaks in Raman spectra, which are symmetry-forbidden in paraelectric SrTiO_3 . Strontium-deficient samples, in particular, exhibit a temperature evolution of Raman spectra consistent with a ferroelectric phase transition

with the transition temperature ~ 350 K. Similar spectra have been recorded from nominally stoichiometric PLD samples proven to be ferroelectric. Our results highlight the sensitive nature of the ferroelectric properties of SrTiO_3 to stoichiometry and imply that strontium deficiency (probably existing in small amounts even in nominally stoichiometric SrTiO_3 films and single crystals) can offer an explanation for the origin of polar nanoregions.

This work was supported in part by the NSF through Grant Nos. DMR-0705127 (D. A. T.), DMR-0507146 (D.G.S.), ECCS-0708759 (C. B. E.), and DMR-0906443 (C. B. E) and through the MRSEC program by DMR-0820404 (C.M.B), DOE EPSCoR Grant No. DE-FG02-04ER46142 (D. A. T.), and Research Corporation for Science Advancement Grant No. 7134 (D. A. T.).

- ¹K. A. Müller and H. Burkard, *Phys. Rev. B* **19**, 3593 (1979).
- ²W. J. Burke, R. J. Pressley, *Solid State Commun.* **9**, 191 (1971).
- ³H. Uwe and T. Sakudo, *Phys. Rev. B* **13**, 271–286 (1976).
- ⁴N. A. Pertsev, A. K. Tagantsev, and N. Setter, *Phys. Rev. B* **61**, R825 (2000).
- ⁵J. H. Haeni, P. Irvin, W. Chang, R. Uecker, P. Reiche, Y. L. Li, S. Choudhury, W. Tian, M. E. Hawley, B. Craigo, A. K. Tagantsev, X. Q. Pan, S. K. Streiffer, L. Q. Chen, S. W. Kirchoefer, J. Levy, and D. G. Schlom, *Nature (London)* **430**, 758 (2004).
- ⁶T. Mitsui, and W. B. Westphal, *Phys. Rev.* **124**, 1354 (1961).
- ⁷J. G. Bednorz and K. A. Müller, *Phys. Rev. Lett.* **52**, 2289 (1984).
- ⁸U. Bianchi, W. Kleemann, and J. C. Bednorz, *J. Phys. Condens. Matter* **6**, 1229 (1994).
- ⁹M. Itoh, R. Wang, Y. Inaguma, T. Yamaguchi, Y. J. Shan, and T. Nakamura, *Phys. Rev. Lett.* **82**, 3540 (1999).
- ¹⁰D. A. Tenne, A. Bruchhausen, N. D. Lanzillotti-Kimura, A. Fainstein, R. S. Katiyar, A. Cantarero, A. Soukiassian, V. Vaithyanathan, J. H. Haeni, W. Tian, D. G. Schlom, K. J. Choi, D. M. Kim, C. B. Eom, H. P. Sun, X. Q. Pan, Y. L. Li, L. Q. Chen, Q. X. Jia, S. M. Nakhmanson, K. M. Rabe, and X. X. Xi, *Science* **313**, 1614 (2006).
- ¹¹D. A. Tenne, P. Turner, J. D. Schmidt, M. Biegalski, Y. L. Li, L. Q. Chen, A. Soukiassian, S. Trolier-McKinstry, D. G. Schlom, X. X. Xi, D. D. Fong, P. H. Fuoss, J. A. Eastman, G. B. Stephenson, C. Thompson, S. K. Streiffer, *Phys. Rev. Lett.* **103**, 177601 (2009).
- ¹²C. M. Brooks, L. Fitting Kourkoutis, T. Heeg, J. Schubert, D. A. Muller, and D. G. Schlom, *Appl. Phys. Lett.* **94**, 162905 (2009).
- ¹³H. W. Jang, A. Kumar, S. Denev, M. D. Biegalski, P. Maksymovych, C. W. Bark, C. T. Nelson, C. M. Folkman, S. H. Baek, N. Balke, C. M. Brooks, D. A. Tenne, D. G. Schlom, L. Q. Chen, X. Q. Pan, S. V. Kalinin, V. Gopalan, and C. B. Eom, *Phys. Rev. Lett.* **104**, 197601 (2010).
- ¹⁴see Supporting Online Material for Tenne *et al.*¹⁰
- ¹⁵W. G. Nilsen and J. G. Skinner, *J. Chem. Phys.* **48**, 2240 (1968).
- ¹⁶P. A. Fleury, J. F. Scott, and J. M. Worlock, *Phys. Rev. Lett.* **21**, 16 (1968).
- ¹⁷A. A. Sirenko, I. A. Akimov, J. R. Fox, A. M. Clark, Hong-Cheng Li, Weidong Si, and X. X. Xi, *Phys. Rev. Lett.* **82**, 4500 (1999).
- ¹⁸J. Petzelt, T. Ostapchuk, I. Gregora, I. Rychetský, S. Hoffmann-Eifert, A. V. Pronin, Y. Yuzyuk, B. P. Gorshunov, S. Kamba, V. Bovtun, J. Pokorný, M. Savinov, V. Porokhonsky, D. Rafaja, P. Vaněk, A. Almeida, M. R. Chaves, A. A. Volkov, M. Dressel, and R. Waser, *Phys. Rev. B* **64**, 184111 (2001).
- ¹⁹D. A. Tenne, I. E. Gonenli, A. Soukiassian, D. G. Schlom, S. M. Nakhmanson, K. M. Rabe, and X. X. Xi, *Phys. Rev. B* **76**, 024303 (2007).
- ²⁰T. Ohnishi, K. Shibuya, T. Yamamoto, and M. Lippmaa, *J. Appl. Phys.* **103**, 103703 (2008).
- ²¹D. J. Keeble, R. A. Mackie, W. Egger, B. Löwe, P. Pikart, C. Hugenschmidt, and T. J. Jackson, *Phys. Rev. B* **81**, 064102 (2010).